MIT Open Access Articles

Genetic Circuit Performance under Conditions Relevant for Industrial Bioreactors

Massachusetts Institute of Technology

Genetic Circuit Performance under Conditions Relevant for Industrial Bioreactors

Felix Moser[1], **Nicolette J. Broers**[2], **Sybe Hartmans**[2], **Alvin Tamsir**[3], **Richard Kerkman**[2], **Johannes A. Roubos**[2], **Roel Bovenberg**[2,4], and **Christopher A. Voigt**[1,*]

[1]Synthetic Biology Center, Department of Biological Engineering, Massachusetts Institute of Technology, Boston, MA 02139 [2]DSM Biotechnology Center, Delft, The Netherlands [3]Tetrad Program, University of California – San Francisco, San Francisco, CA 94158 [4]Synthetic Biology and Cell Engineering, University of Groningen, Groningen, The Netherlands

Abstract

Synthetic genetic programs promise to enable novel applications in industrial processes. For such applications, the genetic circuits that compose programs will require fidelity in varying and complex environments. In this work, we report the performance of two synthetic circuits in *Escherichia coli* under industrially relevant conditions, including the selection of media, strain, and growth rate. We test and compare two transcriptional circuits: an AND and a NOR gate. In *E. coli* DH10B, the AND gate is inactive in minimal media; activity can be rescued by supplementing the media and transferring the gate into the industrial strain *E. coli* DS68637 where normal function is observed in minimal media. In contrast, the NOR gate is robust to media composition and functions similarly in both strains. The AND gate is evaluated at three stages of early scale-up: 100 ml shake-flask experiments, a 1 ml MTP microreactor, and a 10 L bioreactor. A reference plasmid that constitutively produces a GFP reporter is used to make comparisons of circuit performance across conditions. The AND gate function is quantitatively different at each scale. The output deteriorates late in fermentation after the shift from exponential to constant feed rates, which induces rapid resource depletion and changes in growth rate. In addition, one of the output states of the AND gate failed in the bioreactor, effectively making it only responsive to a single input. Finally, cells carrying the AND gate show considerably less accumulation of biomass. Overall, these results highlight challenges and suggest modified strategies for developing and characterizing genetic circuits that function reliably during fermentation.

Keywords

Synthetic Biology; Systems Biology; Genetic Compiler; RBS Calculator; Computer-Aided Design; Fermentation

---

Introduction

There are many potential applications for synthetic genetic programs in biotechnology. One such application is in the development of intracellular controllers for metabolic pathways that integrate environmental and cellular signals, control expression dynamics, and implement feedback loops [1,2]. Such controllers would require multiple circuit modules that can accurately integrate across the complex and dynamic environment of an industrial bioreactor. Many programs that integrate environmental signals and control the dynamics of gene expression have been constructed [3]. However, they have only been shown to operate under ideal, homogeneous conditions at small scales [4-8].

The conditions experienced by cells in large industrial bioreactors are different from those used to characterize circuits in most synthetic biology labs [9]. In bioreactors, cells are grown to high cell densities in oxygen- or carbon-limited conditions [10-12]. Fermentation times can be long and the cells are maintained at low growth rates for extended times [13]. Over the course of fermentation, the metabolic state of the cells goes through phases with different availability of metabolites, redox equivalents, transcription and translation factors, and global regulatory proteins [9, 12, 14-16, 52]. Additionally, not all cells in a large bioreactor are experiencing the same microenvironment due to slow mixing times, causing aeration and local substrate gradients [17-18]. The *E. coli* strains themselves have been optimized for industrial production and are genetically different to those commonly used in synthetic biology [11, 19].

Programs consist of genetic sensors and circuits that have been connected to perform a computational operation. Connecting circuits requires the selection of parts that match the output of an upstream circuit with the input required by a downstream circuit [20-21]. Even slight changes in circuit performance could require the selection of different connecting parts. This poses a challenge when designing programs for environments that differ in conditions from those that were used to characterize the individual circuits. Typically, circuit characterization occurs under lab conditions in shake flasks and complex media. These conditions might differ considerably from the conditions of a program's ultimate application [22]. As programs become larger, it will become impractical to re-characterize each circuit under the precise conditions of the end application before constructing the desired program. Because the process of scale-up occurs in multiple stages, i.e., from shake flask to increasingly larger bioreactors [9, 17], genetic programs need to function reliably under the environmental conditions associated with each stage without the need for additional genetic manipulation.

In this work, we compare the performance of two genetic circuits – an AND gate and a NOR gate – in industrially relevant conditions. Both circuits were characterized previously under lab conditions [21, 22-24]. The two inputs and output of both gates consist of promoters. The AND gate is composed of three plasmids and turns ON when transcription of the Amber suppressor tRNA supD enables the translation of a T7 RNA polymerase (Figure 2). Expression of both SupD and T7 RNA polymerase can have adverse effects on growth [23]. In contrast, the NOR gate is composed of two plasmids and is regulated by two promoters that drive the CI repressor, which has been shown to be non-toxic in many genetic contexts [4, 8, 20, 25]. The choice of these gates enabled us to compare two different circuit architectures that impart different loads on the cell.

The performance of each gate was compared across different environments (Figure 1). First, we tested the impact of changing the composition of the media. Second, we compared the gates' performance in the *E. coli* strain in which the circuits were developed (*E. coli* DH10B) with their performance in a strain used in industry as a model for protein production (*E. coli*

DS68637). Third, we tested the performance of the AND gate during long fermentations and during shifts in the feed rate. Finally, we tested the impact of the choice of RBS strength to connect a genetic sensor to the AND gate during fermentation. Together, these results highlight the challenges of implementing complex genetic circuits in industrial processes and suggest strategies for building circuits for such processes.

Results and Discussion

Media Dependence of the Logic Gates

Media selection for fermentation requires a balance between productive growth and minimizing the cost of components [11, 26]. Complex ingredients, such as yeast extract and tryptone, can boost product formation but are avoided because such components are expensive, complicate product recovery, reduce predictability of fermentations and control over metabolism [11]. To determine the impact of media composition on circuit performance, we characterized each circuit in complex and minimal media in shake flask experiments using the lab strain *E. coli* DH10B (Figure 3).

E. coli DH10B is a common strain for genetic circuit development [21-22, 27]. However, DH10B is a leucine auxotroph and contains the *relA1* and *spoT* alleles, which are known to lower growth rate, especially during nutrient downshifts [28-29]. In LB media, the AND gate exhibits a strong 64-fold induction (Figure 3A). However, in the minimal media the strain does not grow upon induction (Figure S1A). When a small amount (1 g/L) of yeast extract or tryptone is added to supplement growth, the strain grows to saturation, but no AND activity is observed. Activity can be recovered by adding additional yeast extract or tryptone to the minimal medium. The addition of 1 g of either recovers growth when the AND gate is induced, but comparable activity to LB is not observed until 5 g each of tryptone and yeast extract are added.

In contrast, the NOR gate remains functional in all media tested, showing 76-fold induction in LB that is preserved in minimal medium (Figure 3B). Changing the complexity of the media by adding various amounts of tryptone and yeast extract has little effect on either the induced or basal states of the NOR gate. Furthermore, no growth defect is observed in minimal media in either the induced or uninduced state (Figure S1B). The shape and width of the cytometry distributions do not change over these conditions (Figure S3).

Gate Function in an Industrial Strain

E. coli is a common host for the industrial production of recombinant proteins [11, 30-33]. *E. coli* RV308 was first applied to the production of insulin in 1982 and has been used for the production of enzymes, proteases, and therapeutic proteins by Eli Lilly and Merck [31-34]. We examined the activity of the NOR and AND gates in *E. coli* DS68637[†], a modified *E. coli* RV308 variant similar to a strain used at DSM (Methods). Unlike *E. coli* DH10B, the AND gate functions as expected in *E. coli* DS68637[†] in minimal media without the addition of complex ingredients (Figure 4A). However, the output of the induced state is reduced to 26-fold as compared to 64-fold for *E. coli* DH10B grown in LB. The magnitude of the uninduced states is unchanged between media and strains.

We used a standard reference plasmid (pFM46) to compare the absolute ON and OFF states between strains [35]. The fluorescence produced by this reference plasmid is nearly identical across strains and media (Figure 4). While the AND gate function is preserved, the magnitude of the output in the presence of both inducers (+/+) changes between strains. After normalizing to the reference plasmid, this difference is determined to be approximately 7-fold. This could pose a problem when connecting the output of this gate to

downstream devices and could require the selection of a different connecting part, such as a ribosome binding site of a different strength [21].

The NOR gate functions nearly identically in *E. coli* DS68637[†] in minimal medium as in *E. coli* DH10B in LB (Figure 4B). The ON state (-/-) of the gate only differs by 16% between strains. Thus, the NOR gate produces a reliable output irrespective of the strain or media.

Connecting Genetic Circuits: Impact of Media and Strains in Shake-flask

Connecting genetic circuits requires that the output of the upstream circuit matches the input required to activate the downstream circuit [20, 36-37]. A common approach to connect circuits is to vary the ribosome binding site (RBS) sequence downstream of the output promoter [20, 23]. A potential problem could emerge during scale-up when a strain contains a genetic program. If the transfer function of the circuit changes at each stage of scale-up (i.e., is different when measured in a bioreactor compared to shake flask experiments), then this could require a different RBS to functionally connect it to a downstream circuit. If circuits were to require RBS tuning at each stage of scale-up, this would limit the implementation of multi-circuit programs in industrial processes.

In previous work, we analyzed the connection of an arabinose-inducible promoter to an input of the AND gate [21, 23]. We tested multiple RBSs of different strengths and found there was an optimal RBS strength to connect the input promoter to the circuit. Here, a subset of these RBSs is chosen to encompass the transition from functional to non-functional gates (Figure 5). First, we tested whether RBS strength changes as a function of media and strain. Using the J23100 constitutive promoter and RFP reporter, the strength of six RBSs was measured in the context of *E. coli* DH10B in LB and *E. coli* DS68637[†] in minimal medium (Figure S5). RBS strengths were nearly identical across these contexts.

The RBS variants of the AND gate were then tested for their ability to functionally connect the arabinose-inducible promoter to the AND gate (Figure 5). The function of the AND gate is measured for each combination of inducers (-/-, -/+, +/-, +/+) and this is used to assign a "fitness" to the gate. While the magnitude of the output of the gate changes, the rank order of the RBSs is similar. This indicates that while the magnitude of the AND gate changes, the same RBS is optimal in connecting the input promoter to the gate.

Circuit Dynamics in a 1 ml MTP Microreactor

We tested the AND gate in a high-throughput microreactor to assess performance in another context of industrial process development [38]. *E. coli* DS68637 containing the AND gate in different induced states was grown in 2xYT broth for 40 hours (Figure 6A). Differences in the fluorescence of each culture were detected after 3 hours. After 15 hours, no further changes in cell density or fluorescence were observed and remained stable throughout the remainder of the experiment (Figure S6). The AND gate showed partial induction with arabinose (+/-) but was only fully induced in the presence of both inducers (+/+). This partial induction is most likely due to leakiness of the P_{sal} promoter in the absence of salicylate [23]. Correcting this would require a weaker RBS connecting the P_{BAD} promoter to the gate. The absolute magnitude of the output states was compared to the shake flask experiments by comparing expression to the reference plasmid pFM46, which also produced a stable fluorescence per cell culture density in stationary phase (dashed line in Figure 6A).

Circuit Dynamics in a 10 L Bioreactor

The AND gate was tested in a 10 L bioreactor under fed-batch conditions, a common context for process development of industrial recombinant protein production [11, 39]. Variables that indicated circuit performance, including cell density, dry cell weight (DCW),

and fluorescence, were measured after sampling the culture every 3-4 hours (SI section VII). The performance of the AND gate was first measured in *E. coli* DH10B cells (Figure 6B). The culture was maintained in log phase by exponentially increasing the feeding rate (Table S1). The cells were induced after 42 hours by adding both inducers. The AND gate in DH10B only functioned when the feed included a large amount of complex media (100 g/kg yeast extract). Even the addition of 20 g/kg yeast extract to the glucose feed showed no activity when induced.

Next, the industrial strain *E. coli* DS68637 was used to characterize the AND gate in the 10 L bioreactor (Figure 7). As was observed in shake-flask experiments, the addition of yeast extract was not required for AND gate function and did not affect the performance of the gate (Figure S7A). The glucose feed was added at an exponentially increasing rate in order to keep the culture at a constant growth rate. Inducers were added to the cultures 20 hours after exponential feed was initiated. The feed rate was shifted from exponentially increasing to constant 45 hours after addition of the culture [13, 40]. This caused the growth rate to decrease, and cells to undergo a shift from a constant growth rate of 0.05 h^{-1} to very low growth rates. During exponential growth, the circuit rapidly turns on after both inducers are added and the ON state remains stable. In addition, the population of cells is narrow and nearly all of the cells are induced.

However, the circuit breaks late in fermentation. The cell-to-cell variability of the circuit output increases, a significant OFF population appears, and the circuit is almost completely deactivated by the end of fermentation. Plasmid loss assays show that the majority of plasmid is lost by 30 hours (Figure S8). The deactivation of the circuit correlates with the switching of the glucose feed from exponential to constant. An exponential feed rate was started again 70 hours after inoculation to determine if AND gate activity could be rescued by restarting the feed (Figure 7). No significant change in fluorescence was detected after reactivation of exponential feeding, which is consistent with the cells losing their plasmid(s).

The alternative RBSs used to connect the input promoter to the AND gate were also tested in the 10 L bioreactor (Figure 7). The rank order of the RBSs remained the same as compared to the shake flask experiments (Figure 5); however, there are some differences. Notably, RBS_B and RBS_C produce nearly the same induction and RBS_D responds more strongly in the bioreactor (∼10×) than in shake flask experiments (∼2×) (Figure S4). This implies that the arabinose-inducible promoter is producing a higher output, thus requiring a weaker RBS to connect with the gate. Interestingly, the fully-induced state of the RBS_D circuit shows a biphasic distribution with approximately 50% of the cells being induced. Those cells that are in the ON state produce the same output as the stronger RBSs. Thus, when the weaker RBS is used, a subset of the cells is able to properly function, but the remainder exhibits an error that would propagate to a downstream device.

The AND gate containing RBS_B was tested by adding salicylate and then arabinose at a later time point. The addition of salicylate alone is not able to induce the gate (Figure 7). However, the gate is induced with arabinose alone (Figure S7B). This is indicative that the RBS controlling T7 polymerase is too strong and therefore the gate fails and is only responsive to a single input. This implies that the optimum RBS has shifted to be weaker when comparing performance in shake-flask and 10 L bioreactor experiments. This may be predictable based on the microreactor data, where cells only induced with arabinose have an intermediate output between uninduced and fully induced states (Figure 6).

Cells carrying the AND gate accumulate less biomass. The different RBS variants of the AND gate yielded the following biomass accumulation rates: 0.49 g/kg media/hr (RBS_B), 0.56 g/kg media/hr (RBS_C), and 0.64 g/kg media/hr (RBS_D). The rate of cells containing the

reference plasmid is 0.71 g/kg media/hr. Considering the reference plasmid as a control, a single functional AND gate can reduce biomass by as much as 67%. In the microreactor, we observed a similar effect where the induction of the gates caused a lower final OD in the AND gate (Figure S6).

We used a reference plasmid (pFM46) to compare the magnitude of ON and OFF states across strains and growth conditions. The data was normalized to the Kelly reference standard [35] and is reported as Relative Expression Units (REU) (Figure S9, SI Section VI). The reference plasmid was also measured in the microreactor (Figure 6A) and the 10 L bioreactor (Figure 7 and Figure S7B). The fluorescence per cell and the population distribution is fairly stable over the 72 hour fermentation, even after the transition from exponential to constant feed rates (Figure 7). In addition, very little of this plasmid was lost by the end of fermentation (Figure S8). Using the reference plasmid, we calculated the output of the AND gate to be 0.3-3.1 REU in shake-flask experiments, 6.1 REU in the microreactor, and 2.2 REU in a 10 L bioreactor (Figure 8). Therefore, while the circuit is functional under all conditions, the magnitude of the output varies considerably. Notably, the AND gate fails in both the microreactor and 10 L bioreactor in the same way. In both cases, the gate is non-responsive to salicylate and the +/- state is ON when it should be OFF. In the microreactor, it is not a true failure as the +/- state occurs in-between the ON and OFF states in a way that is analogous to fuzzy AND logic (Figures 6, 8). The microreactor is better correlated for the absolute REU measurements, the early detection of a failure mode, and measurements where carrying the circuit impacts the OD (Figure 8). Therefore, it is a better method for predicting the performance of a genetic circuit than shake flask experiments.

Genetic programs can implement computational control over cellular functions, including metabolic processes. They are being applied towards: 1. Controlling the timing of gene expression at different stages of growth, 2. Implementation of feedback, 3. Transfer of process control into individual cells, 4. Consolidation and control of multi-step bio-manufacturing, and 5. Diversification of processing tasks amongst multiple cells. Accomplishing these goals will require increasingly sophisticated programs based on the integration of many circuits.

A challenge in developing genetic programs for an industrial process is the variation that occurs at each stage of scale-up from shake-flask experiments to production-scale bioreactors [9]. Strains and pathways vary in their performance during scale-up and it is expected that similar issues will arise with genetic programs. In this work, we show that a circuit can fail (produce an incorrect computational operation) when moved from shake-flask (uncontrolled batch fermentation) to 10 L bioreactor (controlled fed-batch fermentations at relatively low growth rates) experiments. Further, this circuit exhibits variable responses in industrially-relevant media and strains. To our knowledge, this work represents the first example in which a simple genetic circuit constructed in an academic synthetic biology lab is characterized in the early stages of process scale-up with an industrial partner.

Several efforts are underway to apply high-throughput fabrication to synthesize thousands of genetic parts and circuits [22, 37]. Increasing the throughput will require decreasing the scale at which they are individually characterized, possibly even applying microfluidic screens. A current challenge is designing those assays such that they convey the most valuable information for their incorporation into varied genetic and environmental contexts. As an early step towards this goal, it has been proposed to use a reference construct as a standard for reporting promoter activity [35]. In this work, we found an expression standard to be a useful tool for comparing gate performance at each stage of scale-up and across

industrial and academic labs. We found that the particular promoter-RBS-reporter-backbone choice made by Kelly *et al.* (2009) produces a reliable response in varied environmental contexts. By converting the output to Relative Expression Units (REU), we could quantify a 20-fold variability in the AND gate across environments and labs (an effect that could be qualitatively visualized by eye).

The AND gate contains parts that are toxic and reduce the growth rate [23]. This has a minor impact in shake flask experiments using complex media. However, a notable reduction in the biomass accumulation was observed in 10 L bioreactor experiments. This is particularly problematic considering that desired genetic programs will likely require many integrated circuits. Interestingly, the strength of the RBS connecting a sensor to the AND gate changes the load, where those that yielded the best gates also caused the strongest inhibition of growth. Thus, the optimal RBS has to balance circuit function and growth, a trade-off not previously described.

The microreactor was able to predict one of the failure modes of the AND gate. In the 10 L bioreactor, the gate is not responsive to the salicylate input. This effect was previously observed in shake-flask experiments when the RBS connecting the leaky P_{sal} promoter to the circuit was too strong [21, 23]. Additional sources of failure may have been that the P_{BAD} promoter was stronger or the translation rate of the T7 RNAP gene was higher. The observation of such failure modes due to changes in promoter strength across conditions highlights the need for genetic parts that are insulated from changes in the environment. Although design of such insulation is not yet reliable, some design rules are becoming elucidated [42, 53-55].

Neither the shake-flask nor microreactor experiments were able to predict the rapid decline in output that occurs after the shift from exponential to constant feed rates. The *E. coli* DS68637 strain has been observed to have a lower plasmid copy number [43] and plasmid stability is a problem [44-45]. Indeed, one of the plasmids was rapidly lost after the shift and this resulted in the inactivation of the gate (Figure S8). Such evolutionary instability is a common problem of the plasmid genetics, but it can also be hastened by the presence of toxic parts within a circuit and can depend on the induction state [46]. As technologies for editing the prokaryotic genome expand, unstable plasmid systems such as the ones studied here will be replaced by direct-to-genome programming [47].

In this work, standardized measurements are critical in comparing gate performance across strains, growth conditions, and labs. The wider adoption of standards will enable the more rapid determination of circuit failure modes. Further, it will aid the interpretation of genetic part data gathered at increasingly small scales in fabrication labs and then applied to problems in varied applications, strains, and environments [24, 48]. Even amongst projects within our own lab, and in moving strains between UCSF, MIT, and industrial partners, we have found it challenging to unify the "standardized" measurements made by individual researchers [49-50]. Truly realizing the potential will require the development of large, dedicated consortia of industrial and academic labs.

Methods

Strains and Plasmids

Escherichia coli K-12 RV308 [Su-, lac X 74, gal ISII: OP308, strA] was obtained from ATCC (#31608, deposited by Genentech). The arabinose operon from positions 65,855 to 71,266 (Genbank #U00096) was replaced by the method of Datsenko and Wanner with Kan^R[51] This marker was transduced into the RV308 parent strain by P1 phage (BW28357). Kan^R was then removed using the FRT recombinase encoded by the plasmid

pCP20. The resulting strain was constructed at UCSF to resemble phenotypic characteristics of the DS68637 strain used for fermentation research at DSM. Replicates of shake flask experiments used the strain constructed at UCSF, designated as DS68637[†] in this text. Tube replicates of shake flasks experiments were performed in the Synthetic Biology Center at MIT. All fermentation, microreactor, and initial shake-flask experiments were done with the original DSM DS68637 strain at the DSM Biotechnology Center in Delft.

E. coli DH10B was obtained from Invitrogen (#18297). *E. coli* DH10B and DS68637 (both UCSF and DSM versions) were co-transformed with plasmids pAC-SalSer914, pBR939b, and different RBS variants of pBACr-AraT7940, which together constitute the AND gate [18]. The different RBS variants of pBACr-AraT7940 were designated pFM159, pFM160, pFM161, pFM163, corresponding to RBS_C, RBS_D, RBS_B, and RBS_A, respectively (Table S3). To construct the NOR gate, the strains were co-transformed with plasmid pCI-YFP and plasmid pNOR10-20 [19]. For the RBS variation experiments, Top10 cells (Invitrogen #C4040-10; genetically identical to DH10B) were transformed with RBS plasmids containing a ColE1 replicon bearing the promoter BBa_J23100 (www.partsregistry.org) and a downstream mRFP1 red fluorescent protein [16]. The RBS's driving translation from these constructs were identical to the forward engineered RBSs # 1, 2, 5, 6, 11, and 14 (pFM169-174, respectively) from Salis, et al. (2009) [16]. The reference plasmid pFM46 (Kan^R, p15a) was used as a basis of comparison of reporter expression. This plasmid contains the promoter/RBS/GFP/terminator construct J23102/B0032/E0040/B0015 (www.partsregistry.org) and is nearly identical to the Kelly et al. (2009) standard plasmid [27]. Kelly et al. (2009) used the promoter J23101 as their promoter standard, which is nearly identical in sequence and strength to J23102 [27].

Shake flask and tube Experiments

Plasmids were maintained in shake flasks, the Biolector MTP Microreactor, and the 10 L fermentations by culturing in 10 μg/ml chloramphenicol, 10 μg/ml neomycin, and 50 μg/ml ampicillin. Culturing was done in 2xYT media (Teknova, #Y0167), LB media (Fisher Scientific #R452322), or an in-house defined minimal medium (DSM). The defined minimal medium, which was used in all fermentations and shake flask experiments, was composed of 0.5 % w/w ammonium sulfate, 0.5 % w/w potassium hydrogen phosphate, 3 % w/w MES, 0.4 % w/w glucose, and a proprietary mixture of trace elements. The pH was adjusted to pH 7 before sterilization through a 0.2 μm filter. Yeast extract (BD #212750) and Bacto Tryptone (BD #211705) were added to the defined medium as indicated by adding a stock solution of 50 g/L that had been sterilized by filtration through a 0.2 μm filter. To grow the leucine auxotroph DH10B cultures in minimal media, L-leucine (Acros Organics #12512-1000) was added to the media at 0.5 g/L, which was observed to be sufficient to attain maximal growth rates (data not shown). Induction of AND gates was performed with 1.3 mM L-arabinose (Sigma #A3256) and 0.63 mM sodium salicylate (Sigma #S3007), except as noted. Induction of NOR gates was performed with 1.3 mM L-arabinose (Sigma #A3256) and 100 ng/ml anhydrotetracycline (aTc) (Fluka #37919).

For all experiments reported, *E. coli* cultures frozen in 25% glycerol solution at -80°C were freshly streaked on plates of 2xYT agar and antibiotics. Fresh single colonies from these streaks were then cultured overnight at 37°C and 280 rpm orbital shaking in volumes and media as noted. Both shake flasks and tubes grow cells in oxygen-limited conditions, so forsimplicity, all shake flask and tube replicate experiments are referred to as "shake flask" experiments. For shake flask experiments at DSM, overnight cultures were grown in 20 ml of 2xYT media in 100 ml flasks. After ~18 hours, the OD_{600} of these cultures were measured and they were then diluted back to an OD_{600} of 0.01 in 20 ml of pre-warmed media in 100 ml sterile flask. Shake flask cultures were then grown at 37°C and 280 rpm

orbital shaking. For AND and NOR gate strains, induction occurred at the time of dilution. The cultures were then grown for 18-24 hours prior to measurement. For culture tube experiments at UCSF, all cultures were grown in 14 ml polystyrene culture tubes (Falcon #352059) at 37°C and 280 rpm. Overnight cultures were grown in 3 ml of LB media and antibiotic and were diluted back 1:1000 in 3 ml of media after 18 hours of growth. AND and NOR gate cultures were otherwise treated identically as in DSM shake flask experiments and were then measured by flow cytometry.

At DSM, OD_{600} measurements were performed on an Ultrospec 3100 Pro (Amersham Biosciences) spectrophotometer. At UCSF, OD_{600} measurements were performed on a Cary 50 Bio UV-Vis spectrophotometer (Varian). Cultures were diluted with sterile water until the OD_{600} fell between 0.10 and 0.60, the range across which OD_{600} correlates linearly with cell density.

Flow cytometry

At UCSF, cytometry was done on the BD LSRII flow cytometer and the FACSDiva software as follows. Samples of *E. coli* cultures that were to be measured by cytometry were diluted 1:5 in phosphate buffered saline (PBS) containing 2 mg/ml Kan to stop translation. A 488 nm laser was used for excitation and a 510/20 emission filter was used to measure Forward Scatter, Side Scatter, and GFP fluorescence. A 561 nm laser was used to excite and a 610/20 band pass filter was used to collect RFP fluorescence for RBS library measurements. Events were measured at a flow rate 0.5 μl/s until 50,000 events within the *E. coli* cell population gate were acquired. Analysis of the data was carried out in the FlowJo software package (Treestar). The cell population was gated by the forward and side scatter to include a maximal number of cells (>95%). At DSM, fluorescence was measured using a MoFlo cytometer/cell sorter. During fermentation, aliquots of 8 ml of whole broth was frozen at -20°C. These samples were later thawed and analyzed using the MoFlo cytometer. Upon thawing, each sample was diluted 1:10,000 in PBS and then run on the cytometer. Fresh and frozen samples showed no difference in scatter or fluorescense (data not shown).The 488 nm laser was used for excitation and a 510/20 band pass filter was used to collect GFP fluorescence. The data was exported and analyzed using FlowJo as described above.

Fermentation

Fermentation runs were performed at DSM in cylindrical fermentors with a total volume of 10 L, an internal diameter of 230 mm, two small baffles, and two heat exchangers. Two R6 Rushton turbines stirred the culture. All fermentations were carried out in series of two or three and were performed identically, except as noted (Table S1). The initial 3 L batch phase contained minimal medium with 0.4% w/w glucose, 1% w/w yeast extract, and 0.05% w/w antifoam. A 100 ml shake flask culture was grown on 2xYT media and antibiotics (concentrations as noted above) overnight and used to inoculate the batch phase at $t = 0$. A 3 L feed containing 10% w/w glucose, antibiotics, and supplementary yeast extract as noted was started after the glucose in the batch was exhausted, which occurred roughly 18 hours after inoculation. The initial feed rate was initially 5.5 g/hr, was increased exponentially to maintain a fixed growth rate, and stopped 42 hours after start, after which time the feed rate was kept constant at 45 g/hr. pH was set at 6.8 and was stabilized throughout fermentation by automatic feeds of 10% ammonia and 4 N sulfuric acid. Dissolved oxygen (DO) was initially 100% saturation and was allowed to drop to 50%. Off-gas was analyzed in real-time by mass spectrometry. Profiles of the feed rates, pH, DO, respiratory quotient (RQ), and oxygen consumption rates for the length of each fermentation are reported in Figure S10.

The media for the batch and feed were prepared in fractions and contain the following unless otherwise noted in Table S1. Batch fraction 1 was prepared in a clean fermentor and contained 10 g/kg yeast extract, 2 g/kg K_2HPO_4, and 0.5 g/kg antifoam. Batch fraction 2 contained 4% glucose, 5 g/kg $(NH_4)_2SO_4$, and trace mineral mix (proprietary). Batch fractions 1 and 2 were combined following autoclaving. Feed fraction 1 contained any supplementary yeast extract and salts added to the feed. Feed fraction 2 contained 400 g/kg glucose. Feed fractions 1 and 2 were combined following autoclaving. Antibiotics were prepared in 1000x stock solution, filter sterilized, and added to the batch fraction only (Runs #1-3, Table S1) or the batch fraction and the glucose feed (Runs #4-10, Table S1).

A computer monitored the weight of the glucose feed and the pH titrants, temperature of the culture, and the air input. Temperature of the culture was controlled by a cooling finger and a heat lamp and maintained at 37°C. The dissolved oxygen of the culture was adjusted by controlling the speed of the impellers (Min 200 RPM, Max 750 RPM) and a constant airflow. Samples were taken immediately before addition of the inducers and at accessible time points throughout fermentation. Approximately 50-100 ml of sample were taken from each fermentor at each time point and analyzed. The samples were weighed and the amount was recorded in the central computer, which adjusted the feed rate parameters based on the lost weight. Each sample was then analyzed for culture biomass, OD_{600}, fluorescence, and pH. Three 3 ml aliquots of each sample and the supernatant of each sample were frozen at -20°C for later analysis. OD_{600} measurements of each sample were made in triplicate as described above. GFP fluorescence of each sample was measured by flow cytometry as described. The Dry Cell Weight (DCW) was measured as follows. An aliquot of 10ml of culture was weighed in a 50 ml Falcon conical tube that had been pre-dried at 105°C for 24 hours, diluted with 40 ml of distilled water, and then centrifuged at 6000 rpm for 10 min. The supernatant was poured off, and the pellet in the tube was dried for 24-30 hours at 105°C and weighed. The reported DCW is the weight of the pellet divided by the total weight of the sampled culture.

BioLector Microreactor Experiment

A batch culture of *E. coli* DS68637 carrying the RBS_B AND gate and the reference plasmid (pFM46) were grown in the BioLector CC (m2p labs) instrument using a sterile 48-well flower plate (m2p labs MTP-48-BOH). Each 48-well clear-bottom flower plate had a 1.0 ml capacity/well and contained optodes for monitoring pH and dissolved oxygen. Automated spectrophotometry monitored fluorescence of the entire culture. Culture density was monitored by light scattering and is reported in arbitrary units. One colony from a freshly streaked 2xYT agar plate was used to inoculate a 100 ml culture of the RBS_B AND gate or the reference plasmid. 1 ml of culture was then aliquoted into the 48-well flower plate. Each well of inoculated media contained either no inducer, only one inducer (1.3 mM arabinose or 0.63 mM NaSalicylate), or both inducers. Culture density, fluorescence, pH, and DO were monitored for 40 hours. Additional details of the microfermentation are presented in the Supporting Information.

Supplementary Material

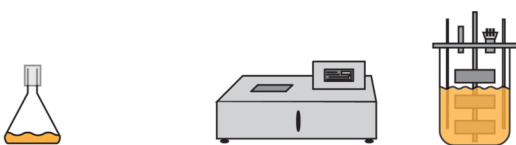Refer to Web version on PubMed Central for supplementary material.

Acknowledgments

References

1. Medema MH, Breitling R, Bovenberg R, Takano E. Exploiting plug-and-play synthetic biology for drug discovery and production in microorganisms. Nat Rev Microbiol. 2011; 9:131–137. [PubMed: 21189477]

2. Anderson JC, Clarke EJ, Arkin AP, Voigt CA. Environmentally controlled invasion of cancer cells by engineered bacteria. J Mol Biol. 2006; 355:619–627. [PubMed: 16330045]

3. Purnick PEM, Weiss R. The second wave of synthetic biology: from modules to systems. Nat Rev. 2009; 10:410–422.

4. Tabor JJ, Salis HM, Simpson ZB, Chevalier AA, Levskaya A, Marcotte EM, Voigt CA, Ellington AD. A synthetic genetic edge detection program. Cell. 2009; 137:1272–1281. [PubMed: 19563759]

5. Lou C, Liu X, Ni M, Huang Y, Huang Q, Huang L, Jiang L, Lu D, Wang M, Liu C, Chen D, Chen C, Chen X, Yang L, Ma H, Chen J, Ouyang Q. Synthesizing a novel genetic sequential logic circuit: a push-on push-off switch. Molecular Systems Biology. 2010; 6:1.

6. Friedland AE, Lu TK, Wang X, Shi D, Church G, Collins JJ. Synthetic gene networks that count. Science. 2009; 324:1199–1202. [PubMed: 19478183]

7. Moon TS, Clarke EJ, Groban ES, Tamsir A, Clark RM, Eames M, Kortemme T, Voigt CA. Construction of a genetic multiplexor to toggle between chemosensory pathways in Escherichia coli. J Mol Biol. 2011; 406:215–227. [PubMed: 21185306]

8. Basu S, Gerchman Y, Collins CH, Arnold FH, Weiss R. A synthetic multicellular system for programmed pattern formation. Nature. 2005; 434:1130–1134. [PubMed: 15858574]

9. Schmidt FR. Optimization and scale up of industrial fermentation processes. Appl Microbiol Biotechnol. 2005; 68:425–435. [PubMed: 16001256]

10. Johnston W, Cord-Ruwisch R, Cooney MJ. Industrial control of recombinant E. coli fed-batch culture: new prospectives on traditional controlled variables. Bioprocess Biosyst Eng. 2002; 25:111–120. [PubMed: 14505011]

11. Lee SY. High cell-density culture of Escherichia coli. TIBTECH. 1994; 14:98–105.

12. Schweder T, Kruger E, Jurgen B, Blomsten G, Enfors SO, Hecker M. Monitoring of genes that respond to process-related stress in large-scale bioprocesses. Biotech & Bioeng. 1999; 65:151–159.

13. Kim BS, Lee SC, Lee SY, Chang YK, Chang HN. High cell density fed-batch cultivation of Escherichia coli using exponential feeding combined with pH-stat. Bioprocess Biosyst Eng. 2004; 26:147–150. [PubMed: 15160725]

14. Han L, Enfors SO, Haggstrom L. Changes in intracellular metabolite pools, and acetate formation in Escherichia coli are associated with a cell-density-dependent metabolic switch. Biotech Lett. 2002; 24:483–488.

15. Klumpp S, Hwa T. Growth rate-dependent partitioning of RNA polymerases in bacteria. Proc Natl Acad Sci. 2008; 105:20245–20250. [PubMed: 19073937]

16. Nomura M. Regulation of ribosome biosynthesis in Escherichia coli and Saccharomyces cerevisiae: diversity and common principles. J Bacteriol. 1999; 181:6857–6864. [PubMed: 10559149]

17. Enfors SO, Jahic M, Rozkov A, Xu B, Hecker M, Jurgen B, Kruger E, Schweder T, Hamer G, O'Beirne D, Noisommit-Rizzi N, Reuss M, Boone L, Hewitt C, McFarlane C, Nienow A, Kovacs T, Tragardh C, Fuchs L, Revstedt J, Friberg PC, Hjertager B, Blomsten G, Skogman H, Hjort S, Hoeks F, Lin HY, Neubauer P, van Der Lans R, Luyben K, Vrabel P, Manelius A. Physiological responses to mixing in large bioreactors. J Biotechnology. 2001; 85:175–185.

18. Hewitt CJ, Boon LA, McFarlane CM. The use of flow cytometry to study the impact of fluid mechanical stress on Escherichia coli W3110 during continuous cultivation in an agitated bioreactor. Biotech & Bioeng. 1998; 59:612–620.

19. Gill RT, DeLisa MP, Valdes JJ, Bentley WE. Genomic analysis of high-cell-density recombinant Escherichia coli fermentation and "cell conditioning" for improved recombinant protein yield. Biotech & Bioeng. 2001; 72:85–94.

20. Yokobayashi Y, Weiss R, Arnold FH. Directed evolution of a genetic circuit. Proc Natl Acad Sci. 2002; 99:16587–16591. [PubMed: 12451174]

21. Salis H, Mirsky EA, Voigt CA. Automated design of synthetic ribosome binding sites to control protein expression. Nature Biotech. 2009; 27:946–951.

22. Baker D, Church G, Collins J, Endy D, Jacobson J, Keasling JD, Modrich P, Smolke C, Weiss R. Engineering Life: Building a FAB for Biology. Scientific American. 2006; 294:44–51. [PubMed: 16711359]

23. Anderson JC, Voigt CA, Arkin AP. Environmental signal integration by a modular AND gate. Molecular Systems Biology. 2007; 3:133. [PubMed: 17700541]

24. Tamsir A, Tabor JJ, Voigt CA. Robust multicellular computing using genetically encoded NOR gates and chemical 'wires'. Nature. 2010; 212:212–215. [PubMed: 21150903]

25. Rosenfeld N, Young JW, Alon U, Swain PS, Elowitz MB. Accurate prediction of gene feedback circuit behavior from component properties. Molecular Systems Biology. 2007; 3:143. [PubMed: 18004276]

26. Weuster-Botz D. Experimental design for fermentation media development: Statistical design or global random search? J Bioscience and Bioengineering. 2000; 90:473–483.

27. Pfleger BF, Pitera DJ, Smolke CD, Keasling JD. Combinatorial engineering of intergenic regions in operons tunes expression of multiple genes. Nat Biotech. 2006; 24(8):1027–1032.

28. Durfee T, Nelson R, Baldwin S, Plunkett G III, Burland V, Mau B, Petrosino JF, Qin X, Muzny DM, Ayele M, Gibbs RA, Csorgo B, Posfai G, Weinstock GM, Blattner FR. The Complete Genome Sequence of Escherichia coli DH10B: Insights into the Biology of a Laboratory Workhorse. J Bacteriol. 2008; 190:2597–2606. [PubMed: 18245285]

29. Cox JM, Li H, Wood EA, Chitteni-Pattu S, Inman RB, Cox MM. Defective dissociation of a "slow" recA mutant protein imparts an Escherichia coli growth defect. J Biol Chem. 2008; 283(36):24909–24921. [PubMed: 18603529]

30. Becker GW, Hsiung HM. Expression, secretion and folding of human growth hormone in Escherichia coli. FEBS. 1986; 204:145–150.

31. Wetzel R, Kleid DG, Crea R, Heyneker HL, Yansura DG, Hirose T, Kraszewaki A, Riggs AD, Itakura K, Goeddel DV. Expression in Escherichia coli of a chemically synthesized gene for a "mini-C" analog of human proinsulin. Gene. 1981; 16:63–71. [PubMed: 7044895]

32. Horn U, Strittmatter W, Krebber A, Knupfer U, Kujau M, Wenderoth R, Muller K, Matzku S, Pluckthum A, Riesenberg D. High volumetric yields of functional dimeric miniantibodies in Escherichia coli, using an optimized expression vector and high-cell-density fermentation under non-limited growth conditions. Appl Microbiol Biotechnol. 1996; 46:524–532. [PubMed: 9008885]

33. Belagaje RM, Reams SG, Ly SC, Prouty WF. Increased production of low molecular weight recombinant proteins in Escherichia coli. Protein Science. 1997; 6:1953–1962. [PubMed: 9300495]

34. Birch GM, Black T, Malcolm SK, Lai MT, Zimmerman RE, Jaskunas SR. Purification of recombinant human rhinovirus 14 3C protease expressed in Escherichia coli. Protein Expression and Purification. 1995; 6:609–618. [PubMed: 8535153]

35. Kelly JR, Rubin AJ, Davis JH, Ajo-Franklin CM, Cumbers J, Czar MJ, de Mora K, Glieberman AL, Monie DD, Endy D. Measuring the activity of BioBrick promoters using an in vivo reference standard. J Biol Eng. 2009; 3:1–13. [PubMed: 19118500]

36. Clancy K, Voigt CA. Programming Cells: Towards an automated 'Genetic Compiler'. Curr Opin Biotech. 2010; 21:1–10. [PubMed: 20189376]

37. Carothers JM, Goler JA, Juminaga D, Keasling JD. Model-Driven Engineering of RNA Devices to Quantitatively Program Gene Expression. Science. 2011; 334:1716–1719. [PubMed: 22194579]

38. Huber R, Roth S, Rahmen N, Büchs J. Utilizing high-throughput experimentation to enhance specific productivity of an E.coli T7 expression system by phosphate limitation. BMC Biotechnol. 2011; 11:1–11. [PubMed: 21208406]

39. Johnston W, Cord-Ruwisch R, Cooney MJ. Industrial control of recombinant E. coli fed-batch culture: new perspectives on traditional controlled variables. Bioprocess Biosyst Eng. 2002; 25:111–120. [PubMed: 14505011]

40. Pan JG, Rhee JS, Lebeault JM. Physiological constraints of in increasing biomass concentration of Escherichia coli B in fed-batch culture. Biotechnology Letters. 1987; 9:89–94.

41. Hewitt CJ, Boon LA, McFarlane CM. The use of flow cytometry to study the impact of fluid mechanical stress on Escherichia coli W3110 during continuous cultivation in an agitated bioreactor. Biotech & Bioeng. 1998; 59:612–620.

42. Sasson V, Shachrai I, Bren A, Dekel E, Alon U. Mode of Regulation and the Insulation of Bacterial Gene Expression. Mol Cell. 2012; 46:399–407. [PubMed: 22633488]

43. Lancaster MJ, Sharp RJ, Court JR, McEntee ID. Production of cloned carboxypeptidase G2 by Escherichia coli: Genetic and environmental considerations. Biotechnology Letters. 1989; 2:699–704.

44. Cooper N, Brown ME, Caulcott CA. A mathematical method for analysing plasmid stability in micro-organisms. J Gen Microb. 1987; 133:1871–1880.

45. Kumar PKR, Maschke HE, Friehs K, Schugert K. Strategies for improving plasmid stability in genetically modified bacteria in bioreactors. TIBTECH. 1991; 9:279–284.

46. Andersson L, Yang S, Neubauer P, Enfors SO. Impact of plasmid presence and induction on cellular responses in fed batch cultures of Escherichia coli. J Biotechnology. 1996; 46:255–263.

47. Tyo KEJ, Ajikumar PK, Stephanopoulos G. Stabilized gene duplication enables long-term selection-free heterologous pathway expression. Nature Biotech. 2009; 27(8):760–763.

48. Canton B, Labno A, Endy D. Refinement and standardization of synthetic biological parts and devices. Nat Biotech. 2008; 26:787–793.

49. Temme K, Zhao D, Voigt CA. Refactoring the nitrogen fixation gene cluster from Klebsiella oxytoca. Proc Natl Acad Sci. 2012; 109(18):7085–90. [PubMed: 22509035]

50. Moon TS, Lou C, Tamsir A, Stanton BC, Voigt CA. Genetic programs constructed from layered logic gates in single cells. Nature. 2012 Advanced online publication. 10.1038/nature11516

51. Datsenko KA, Wanner BL. One-step inactivation of chromosomal genes in Escherichia coli K-12 using PCR products. Proc Natl Acad. 2000; 97(12):6640–6645.

52. Weber H, Polen T, Heuveling J, Wendisch VF, Hengge R. Genome-wide analysis of the general stress response network in Escherichia coli: sigmS-dependent genes, promoters, and sigma factor selectivity. J Bacteriol. 2005; 187:1591–1603. [PubMed: 15716429]

53. Davis JH, Rubin AJ, Sauer RT. Design, construction, and characterization of a set of insulated bacterial promoters. Nucleic Acids Res. 2011; 39(3):1131–1141. [PubMed: 20843779]

54. Lou C, Stanton B, Chen YJ, Munsky B, Voigt CA. Ribozyme-based insulator parts buffer synthetic circuits from genetic context. Nat Biotech. 2012 Advanced online publication. 10.1038/nbt.2401

55. Qi L, Haurwitz RE, Shao W, Doudna JA, Arkin AP. RNA processing enables predictable programming of gene expression. Nat Biotech. 2012 Advanced online publication. 10.1038/nbt.2355

Gate:	NOR	AND	AND	AND
Tested Parameters	Media dependence Strain dependence Population variability	Media dependence Strain dependence Part selection Population variability	Microreactor growth	Media dependence Strain dependence Part selection Population variability Feed rate dependence

Figure 1. Overview of Experiments
The NOR gate and AND gate are compared across media and strains in shake flask experiments. The AND gate is further characterized in an MTP microreactor and 10 L bioreactor.
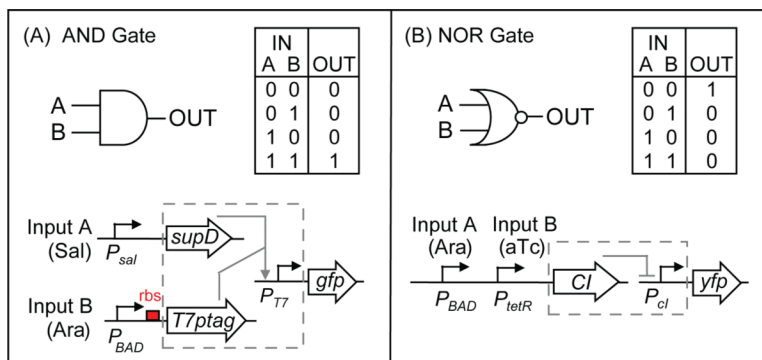
Figure 2. The Genetic AND and NOR Gates
The symbol, look-up table, and structure of the genetic logic gates are shown. **(A)** The AND gate is based on a variant of T7 polymerase that contains two Amber stop codons (T7ptag). Only when the tRNA Amber suppressor SupD is transcribed is the T7 polymerase translated and turns ON the output T7 promoter driving the GFP reporter. The RBS varied in this study is shown in red. **(B)** The NOR gate is based on two tandem promoters that drive the expression of a repressor (CI) that turns off an output promoter driving the GFP reporter.
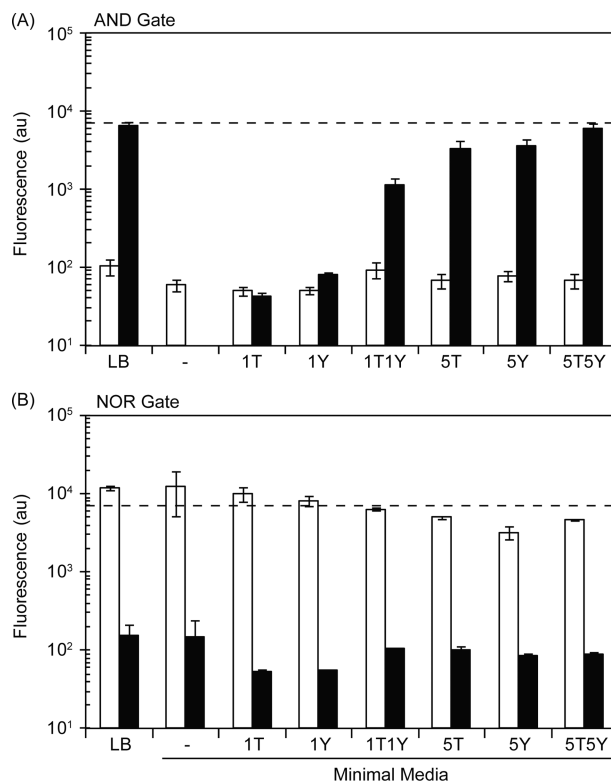
Figure 3. Impact of Media on Gate Performance in *E. coli* DH10B

Media composition affects the performance of the AND (RBS$_B$) and NOR gates. *E. coli* DH10B carrying the **(A)** AND or **(B)** NOR gate were grown both uninduced (white bars) and induced (black bars) in media of varying composition. The media composition is listed below the data. LB-Miller (LB) contains 10 g/L Tryptone, 5 g/L yeast extract, and 10 g/L NaCl. The other media is either unsupplemented minimal media (-) or minimal media supplemented as follows: 1 g/L Yeast Extract (1Y), 1 g/L Tryptone (1T), 5 g/L yeast extract (5Y), 5 g/L Tryptone (5T), 1 g/L yeast extract + 1 g/L Tryptone (1Y1T), 5 g/L yeast extract + 5 g/L tryptone (5Y5T). The output of the reference plasmid pFM46 (dotted line) is shown for comparison. All cultures were measured after 9 hours, except the cultures that were grown on minimal (unsupplemented) media, which were measured after 24 hours. Induced AND gates never grew on minimal media. The error bars represent the standard deviation of three experiments performed on different days.
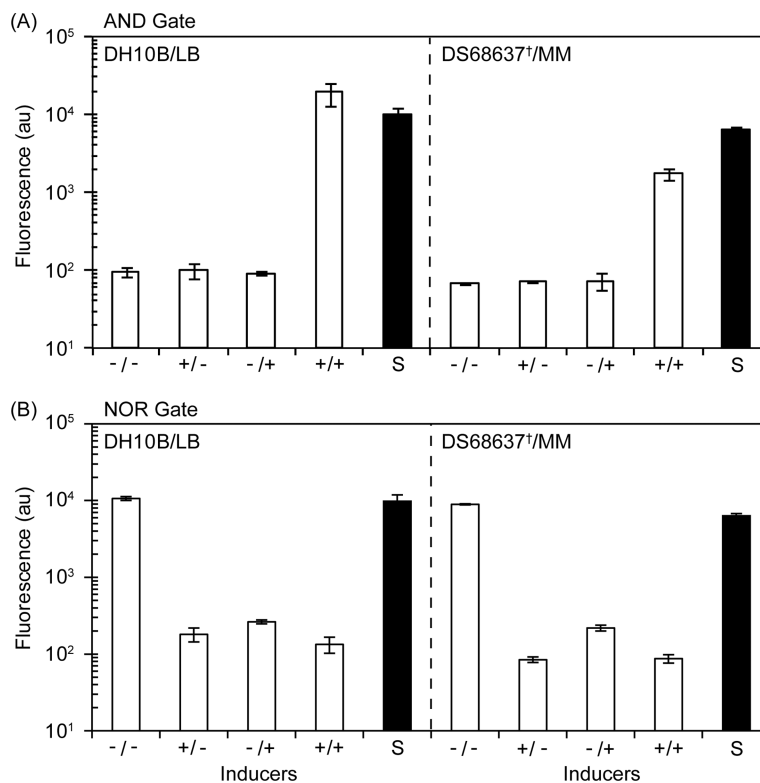
Figure 4. Comparison of Gate Performance in *E. coli* DH10B and *E. coli* DS68637[†]
Gate performance is measured in DH10B grown on LB and in DS68637[†] grown on
unsupplemented minimal media (MM). **(A)** The output of the AND gate (RBS_B) is shown
for four combinations of inputs: -/- (no inducers), +/- (1.3 mM arabinose), -/+ (0.63 mM
salicylate), +/+ (both inducers). The output of the reference plasmid pFM46 (S, black bars)
is shown for both strain/media combinations. **(B)** The output of the NOR gate is shown for
four combinations of inputs: -/- (no inducers), +/- (1.3 mM arabinose), -/+ (100 ng/ml aTc),
+/+ (both inducers). In *E. coli* DH10B, the AND gates were measured after 9 hours and
NOR gates were measured after 24 hours according to previously established protocols [21,
23]. In DS68637[†], the AND and NOR gates were both measured after 24 hours due to
slower growth on the minimal media. The error bars represent the standard deviation of
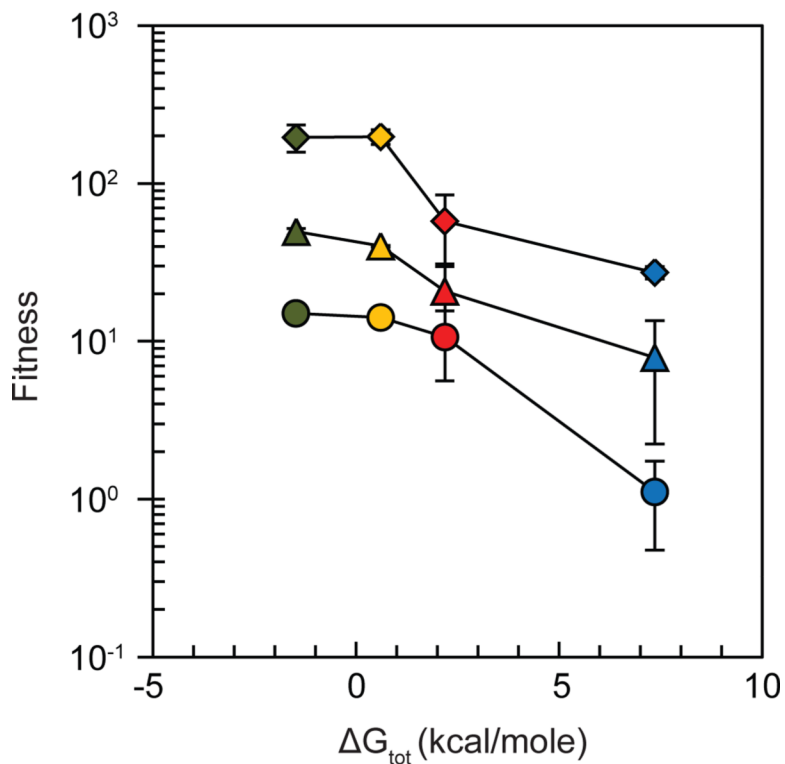three experiments performed on different days.

Figure 5. Media and Strain Impact on RBS selection
The effect of varying the strength of the RBS connecting the arabinose sensor to the AND gate is shown. The ΔG_{tot} is the strength of the RBS as determined using a biophysical model [21]. A more positive ΔG_{tot} predicts strong secondary structure formation around the RBS, which correlates strongly with weaker translation [21]. Fitness scores the accuracy and function of the gate in each condition. A higher fitness indicates that the circuit is properly performing the AND function. The fitness was calculated as follows: First, the baseline fluorescence (-/-) was subtracted from each state. Then, the fluorescence of all states were normalized to the highest value of a partially induced state (-/+, +/-). Finally, the partially induced states were subtracted from the ON state (+/+). The RBSs characterized in this manuscript are colored (RBS$_A$: green, RBS$_B$: orange, RBS$_C$: red, and RBS$_D$: blue) and were previously characterized [18]. The calculated fitness is shown for the four RBS's studied for different media and strains. The media are LB broth (diamonds), minimal media containing 5 g/L yeast extract (5Y, triangles), and unsupplemented minimal media (circles). *E. coli* DH10B was measured in LB and 5Y, and *E. coli* DS68637[†] was measured in unsupplemented minimal medium. Error bars represent 1 standard deviation of three experiments.
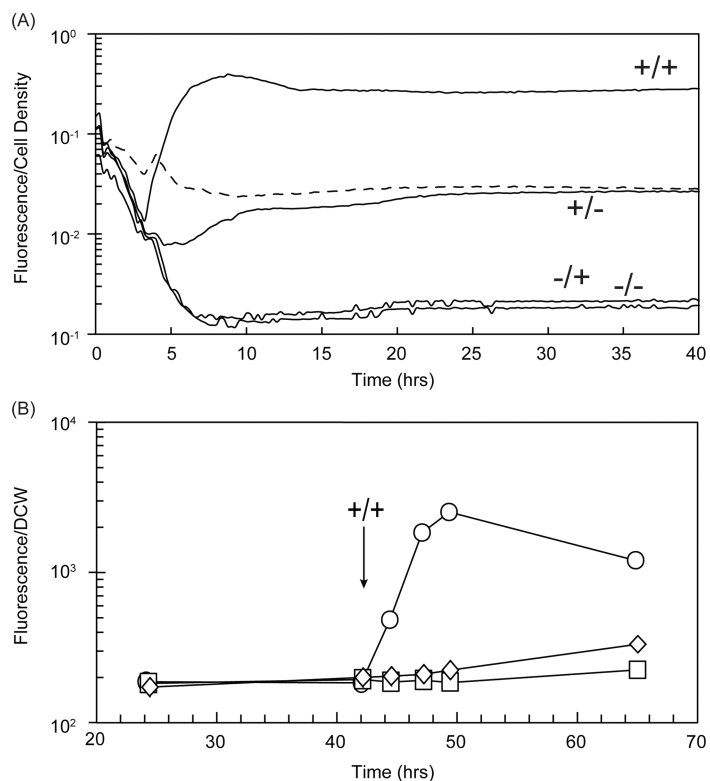
(A)

(B)

Figure 6. Performance of an AND gate and Reference Plasmid in a Microreactor and 10 L Bioreactor

Cultures of *E. coli* DS68637 carrying the RBS$_B$ AND gate and a reference plasmid (pFM46) were grown in a BioLector microreactor on a 1 ml batch of rich 2xYT medium. **(A)** Cultures were induced at time 0 with either no inducer (-/-), single inducers (+/-, arabinose only; -/+ salicylate only) or both inducers (+/+). The fluorescence, cell density, dissolved oxygen, and pH of each culture was monitored for 40 hours (Figure S6). The reference plasmid data is shown as a dashed line. **(B)** The performance of *E. coli* DH10B carrying the RBS$_B$ AND gate is shown in a 10 L bioreactor. Both inducers (1.30 mM arabinose and 0.63 mM salicylate) are added at 42.5 hours. The fluorescence per dry cell weight (DCW) is shown for three fermentations in which the amount of yeast extract in the feed is varied: 0 g/kg (squares), 20 g/kg (diamonds), and 100 g/kg (circles). The glucose feed is initiated at 15 hours after inoculation and is exponentially increased over the course of the fermentation.
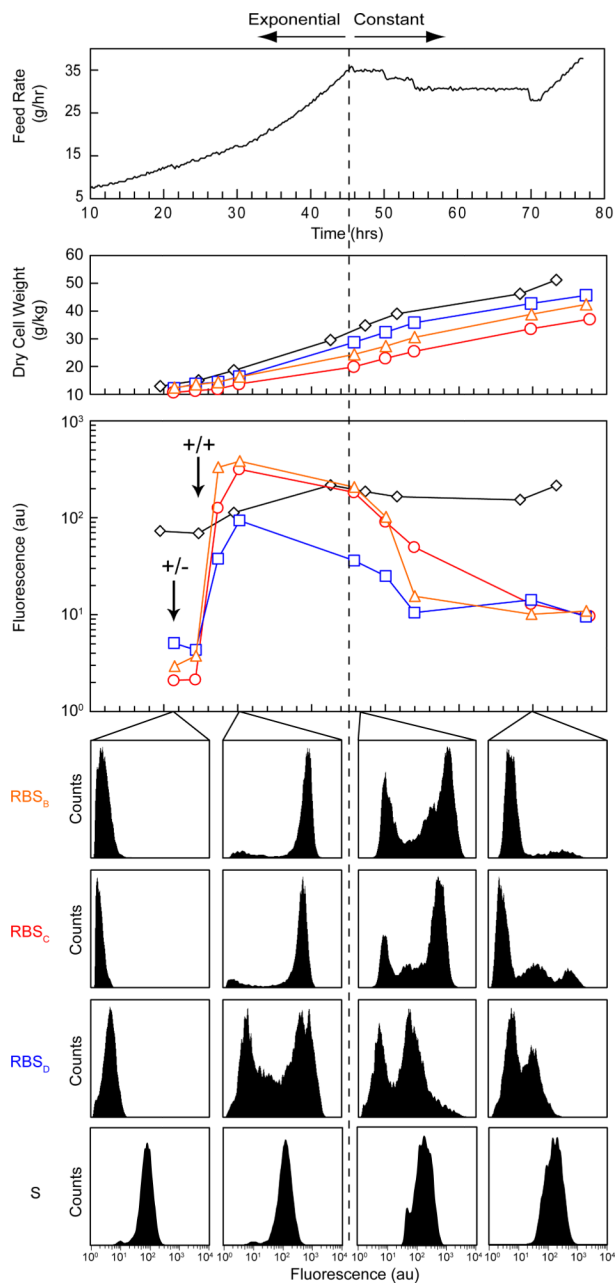
Figure 7. Performance in Fermentation of AND Gate RBS Variants
Three fermentations of RBS variants of the AND gate in *E. coli* DS68637 were performed. AND gate variants included either a strong (RBS$_B$, orange triangles), medium (RBS$_C$, red circles), and weak (RBS$_D$, blue squares) RBS, which correspond in color to RBS's tested in Figure 5. These three fermentations were performed identically, with changes in feed rate and DO made as needed to match growth rates of the cultures. AND gate cultures were induced at 21 hours with 0.63 mM sodium salicylate (+/-) and then with 1.3 mM arabinose (+/+) at 24 hours. The feed rate was exponentially increased until 45 hours and then switched to a fixed feed rate; the dotted line marks the time of the switch. Samples were taken at 9 different times throughout fermentation. Dry cell weight (DCW) and fluorescence of each culture were measured at each time point. Fluorescence cytometry distributions are shown for the circuit in the OFF state (21 hours), when fully induced (30 hours),

immediately after the shift to constant feeding (46 hours), and after 70 hours. For comparison, performance of an *E. coli* DS68637 strain carrying the reference plasmid pFM46 (S; black diamonds) is shown. The reference plasmid fermentation was carried out on a separate day and was sampled at 20, 30, 47, and 68 hours after inoculation. Data for this figure was gathered from Runs #6-8 for the AND gates and from Run #11 for the reference plasmid (Figure S7B, Table S1).
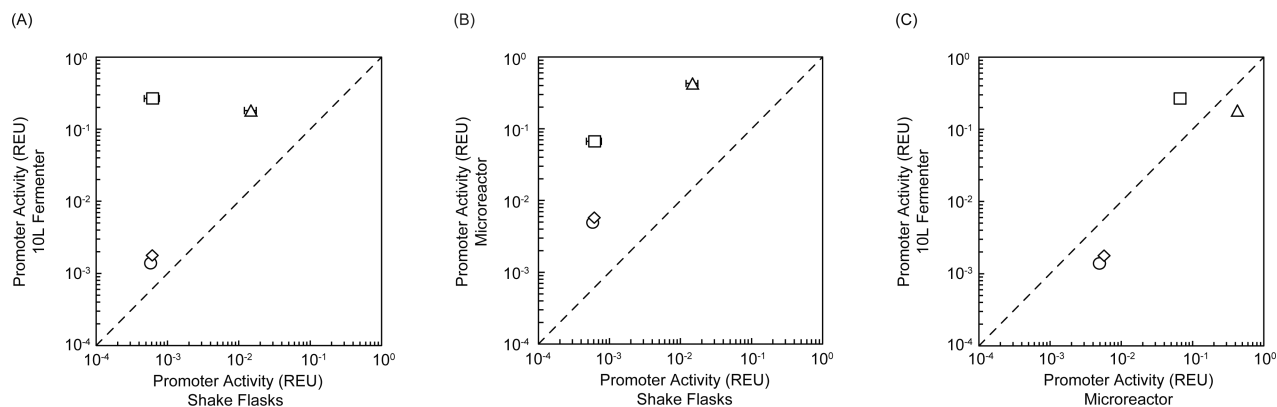
(A)

(B)

(C)

Figure 8. Comparison of AND gate activity across growth conditions
To compare AND gate expression across different growth conditions (shake flasks, 1 ml microreactor, and 10 L bioreactor), GFP fluorescence output of the RBS$_B$ AND gate was converted to relative expression units (REU) defined by the Kelly standard plasmid (SI Section VIII). This relative expression of the AND gate is compared in each pair of the following conditions: **(A)** shake flasks versus 10 L bioreactor, **(B)** shake flasks versus 1 ml MTP microreactor, and **(C)** 1 ml MTP microreactor versus 10 L bioreactor. The four different states (-/-, circles; ara/-, squares; -/sal, diamonds; +/+, triangles) are plotted. The dotted line represents a theoretically perfect correlation between states. The shake flask cultures are unable to predict the ara/-failure mode in the 1 ml microreactor and the 10 L bioreactor. However, the 1 ml microreactor predicted the ara/- failure mode of the gate in the 10 L bioreactor. Data for the shake flask cultures is taken from DS68637[†] grown on unsupplemented minimal media (Figure 4). The data for the microreactor corresponds to the mean fluorescence of each culture between 10 and 40 hours in Figures 6A and S6. Data for the 10 L bioreactor are derived from Run #6 (-/-, -/sal, +/+; Table S1) and Run #9 (ara/-; Figure S7B).